Surface Chemistry

DOI: 10.1002/anie.200800810

Micrometer-Scale Protein-Resistance Gradients by Electron-Beam Lithography**

Tobias Winkler, Nirmalya Ballav, Heidi Thomas, Michael Zharnikov, and Andreas Terfort**

Gradients are an inherent feature of biology. They are a cause for orientational and translational phenomena, such as phototaxis or chemotaxis, and can be used to generate energy or vital substances. On surfaces, concentration gradients direct the morphogenesis, the alignment, or even the migration of cells (haptotaxis), and thus are of central importance. Typical haptomers are adhesion proteins, whose surface concentration gradients can lead to the desired behavior. It is generally assumed that a cell needs to sense a concentration difference of 2–10% between its leading edge and the rear side to express a suitable biological response.[1] As typical cellular dimensions amount from 2 μm (bacteria) to 20 μm (eukaryotic cells), it is of interest to fabricate relatively steep surface gradients of protein concentration, calling for innovative methods of micro- and nanotechnology.[2]

Self-assembled monolayers (SAMs) are a very useful tool to adjust surface properties. Many methods have been established to obtain chemical gradients based on SAMs, typically by mixing two kinds of molecules, either in a one-step or two-step manner using, for example, electrochemical potential gradients,[3,4] time-controlled exposure,[5] diffusion-controlled microcontact printing,[6] or interdiffusion involving either gas-phase diffusion,[7,8] or gels.[9,10] These methods are inherently useful for the centimeter or millimeter scale, thus only allowing very shallow gradients to be produced. The use of microfluidic setups allowed the reduction of the gradients down to a couple of micrometers, thus making them steeper, but also carried severe restrictions on the available patterns.[11,12] Other methods involve the use of electrochemical scanning tunneling microscopy,[13] or UV light either for the gradual degradation[14,15] or extension[16] of SAMs; they are also mostly limited to certain patterns and/or size domains.

Herein we present a method to form gradients of bioresistance down to the micrometer scale using the irradiation-promoted exchange reaction (IPER) and self-assembled monolayers (SAMs) as the primary template.[17–19] We and others have demonstrated in the past that SAMs of thiolates on gold can be affected by either X-rays,[20,21] UV

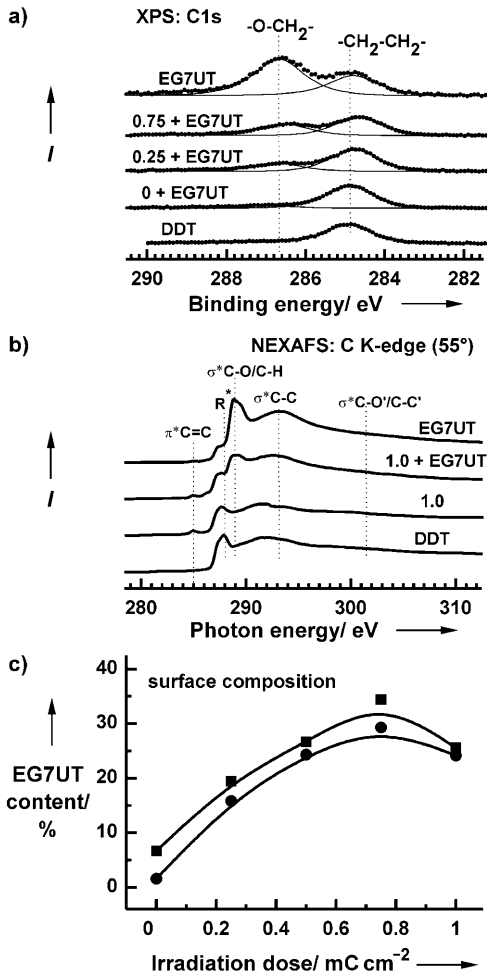

Figure 1. a) C 1s XP spectra and b) C K edge NEXAFS spectra (angle of incidence 55°) of DDT SAMs which were either irradiated (only NEXAFS) or subsequently irradiated (variable dose) and immersed into EG7UT/EtOH solution for 2 h. For comparison, the spectra of pristine DDT and EG7UT SAMs and the C 1s spectrum of DDT/Au immersed into EG7UT/EtOH solution for 2 h (without irradiation) are also depicted. The irradiation doses (in mC cm^{-2}) are given at the respective curves. (c) The relative composition of the mixed SAMs derived from the C 1s (■) and O 1s (●) XP spectra.

[*] N. Ballav, Dr. M. Zharnikov
Angewandte Physikalische Chemie
Universität Heidelberg
69120 Heidelberg (Germany)
Fax: (+49) 6221-546-199
E-mail: Michael.Zharnikov@urz.uni-heidelberg.de
T. Winkler, H. Thomas, Prof. Dr. A. Terfort
Fachbereich Chemie
Universität Marburg
35032 Marburg (Germany)
Fax: (+49) 6421-282-5690
E-mail: aterfort@chemie.uni-marburg.de

[**] T.W., N.B., and H.T. contributed equally to this work. This work has been financially supported by the DFG (ZH 63/9-2 and Te 247/6-2). N.B. and M.Z. thank M. Grunze for support of this work, S. Schilp for the help with electron-beam lithography, C. Wöll for the technical cooperation at BESSY II, and the BESSY II staff for their assistance.

Supporting information for this article is available on the WWW under http://dx.doi.org/10.1002/anie.200800810.

exposure,[22,23] or electron irradiation,[18,24–26] resulting in the appearance of conformational and orientational defects and bond cleavage. The affected molecules can be relatively easily desorbed or displaced by other species capable of binding on the same substrate, resulting in a mixed SAM. The extent of exchange reaction, that is, the composition of the resulting SAM, can be gradually varied by selection of a proper irradiation dose. We were interested in combining IPER with electron-beam lithography (EBL) and test if gradients of bioresistance can be obtained in this way. Of particular interest is the reduction of the spatial dimensions of the gradient to cellular dimensions (several micrometers), as the gradients might otherwise be too shallow to be sensed by single cells.

To examine the possibility to vary bioresistance gradually by IPER, we started with control experiments on uniform SAM samples. Dodecanethiolate SAMs (DDT SAMs) on gold were prepared and irradiated by electrons (10 eV) with a variable dose under UHV conditions. Then the exchange reaction with a heptaethylene glycol terminated undecanethiol ($HO(CH_2CH_2O)_7(CH_2)_{11}SH$, EG7UT), a molecule known to form monolayers resistant to the adsorption of proteins, was performed by immersion into an ethanolic solution of EG7UT for 2 h. The resulting monolayers were characterized by X-ray photoelectron spectroscopy (XPS) and near-edge X-ray absorption fine structure spectroscopy (NEXAFS). XPS provides a good means to follow the exchange process, as the C 1s emission of carbon atoms in an alkane chain ($C-CH_2-C$) can be clearly distinguished from that of carbon atoms in the ethylene glycol (EG) part of the bioresistant molecules ($O-CH_2-C$). Figure 1 a shows the C 1s XP spectra of pristine DDT and EG7UT monolayers, and the spectra of DDT monolayers processed by IPER with EG7UT as the substituent. Without irradiation, the exchange reaction occurs to a very small extent only. In contrast, it takes place to a controlled level upon irradiation: With increasing electron dose, the amount of incorporated EG7UT increases up to a certain level (about 30%, see Figure 1 c), from which on the substitution is hampered. The same conclusions can be deduced from the O 1s XP spectra (see the Supporting Information) and the C K edge NEXAFS spectra shown in Figure 1 b.

The C K edge NEXAFS spectra, in addition, give a hint about the primary processes behind IPER. The observed saturation behavior can be rationalized by two competing processes induced by the electrons: 1) The kinetically faster process involves the cleavage of C–H, C–C, and S–Au bonds and the appearance of conformational and orientational defects.[26] This effect results in diminished attachment of the affected molecules to the substrate and weaker intermolecular interactions with their neighbors. Thus, these molecules can be relatively easy replaced by the substituent molecules in the following, wet-chemical step.[18] 2) The slower process, which is prominent at higher doses, is the cross-linking of the SAM constituent by intermolecular C–C bond formation,[26] which hinders the exchange by substituents[18] as schematically shown in Figure 2, where the cases of the undamaged monolayer and the exchange reaction after electron irradiation with a low dose are also presented. In the following, we will refer to the aftermath of the exchange reaction and call the nonirradiated SAM phase A (shown in red), the SAM for which a positive relation exists between the dose and the extent of the substitution phase B (green), and the cross-linked film phase C (yellow).

To test for the bioresistance of the surfaces obtained by the consecutive irradiation/immersion process, we used the adsorption of proteins as a model system (cell experiments will follow). A significant dependence of the protein-layer thickness on the irradiation dose is found (Figure 3). At small doses, the surface becomes more and more protein-resistant,

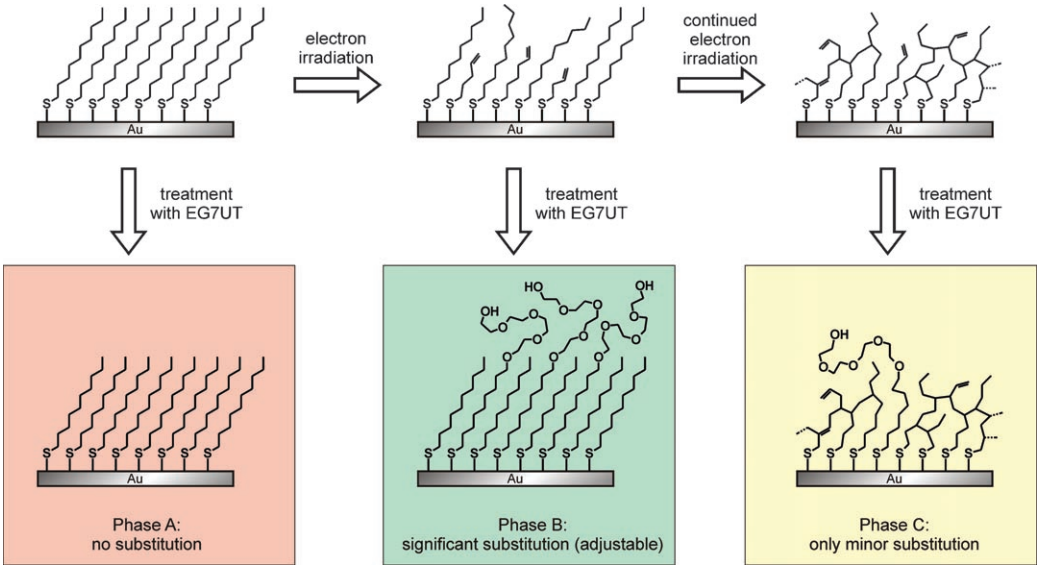

Figure 2. The molecular mechanism of the IPER process. Whereas the pristine DDT SAM hardly permits any substitution by EG7UT (phase A, red), the appearance of irradiation-induced defects promotes the exchange reaction with EG7UT molecules (phase B, green). Upon prolonged irradiation, cross-linking between the molecules becomes significant, hindering to some extent the exchange reaction (phase C, yellow). The color coding is used in the following figures to illustrate the different phases.

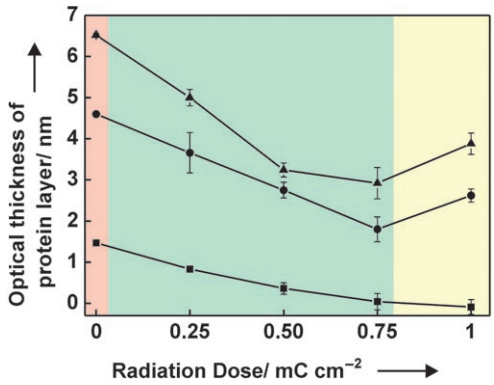

Figure 3. The thickness of the adsorbed protein films on the IPER-engineered templates as functions of irradiation dose (10 eV electrons): ■ BSA, ● globulin, ▲ fibrinogen. The minimum at about 0.75 mC cm^{-2} in the fibrinogen and globulin curves indicates the transition from phase B to phase C. See Figure 1 c for the composition of the templates.

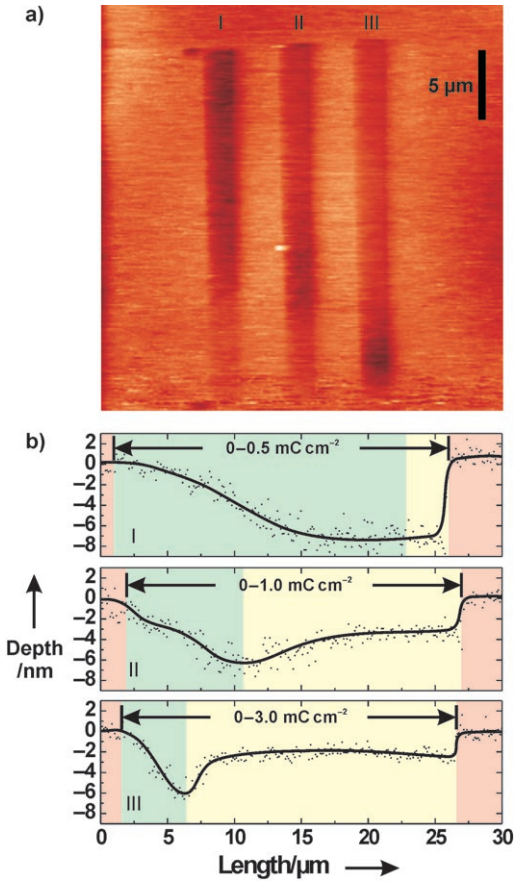

Figure 4. a) An AFM image of the protein-gradient micropattern taken after the adsorption of fibrinogen on the DDT/EG7UT template fabricated by a combination of IPER and EBL. The irradiation dose along the stripes was gradually varied from 0 to 0.5 (I), 1.0 (II), and 3.0 mC cm^{-2} (III). b) Height profiles along the protein gradient stripes (the lines are a guide to the eye). The adsorption of the proteins clearly follows the gradient of EG7UT concentration in the DDT/EG7UT template. The stripes appear as depressions as the nonirradiated matrix (pristine DDT SAM) is covered by a thick layer of protein.

until an optimum is reached at about 0.75 mC cm^{-2}, but complete protein resistance could only be obtained for the frequently used bovine serum albumin (BSA). The two others proteins, fibrinogen and γ-globulin, are obviously much more adhesive, so that the thicknesses of the respective layers could only be reduced to about 45 % of the value found on pristine DDT SAM. This value is in excellent agreement with the results obtained by Prime and Whitesides, who exposed mixed monolayer systems containing undecanethiol and the somewhat shorter EG6UT to different proteins: A monolayer containing 30 % of EG6UT (comparable to the EG7UT content obtained after an area dose of 0.75 mC cm^{-2}) formed fibrinogen adlayers with about half the thickness as obtained on pure undecanethiol SAMs.[27]

Mixed monolayers obtained either by immersion in a solution containing both thiols,[27] or by interdiffusion of the components have (at least) two inherent constraints: no spatial control of the composition is possible, and the molecules might segregate into domains on the surface. In contrast, mixed DDT/EG7UT films fabricated by IPER are presumably characterized by a homogenous mixture of DDT and EG7UT as the irradiation-induced defects, promoting the exchange, are stochastically distributed over the film. Furthermore, the irradiation process permits the local adjustment of the exchange efficiency—and thus the resulting protein affinity—on different length scales down to the size of cells, namely, a couple of micrometers.

We combined IPER with EBL and used a focused electron beam (1 keV) in a scanning electron microscope with a pattern generator system to lithograph gradient-like lines into DDT layers, with the subsequent development of the fabricated pattern by the exchange reaction with EG7UT as described above. The microgradients were then exposed to the protein solutions to determine the affinity behavior. The lithographed stripes, with a length of 25 µm and a width of 3 µm, are clearly visible in AFM micrographs (Figure 4 a) as trenches in an environment otherwise fully covered by protein (pristine DDT SAM; phase A). A striking feature is an obvious dip located at different places along the trenches, resulting from different dose gradients used in lithographing these stripes. The lowest protein affinity can be found at places exposed to a dose of about 0.3 mC cm^{-2} (Figure 4 b). This is about a factor of 2.5 smaller than the optimal dose found in the experiments on the uniform SAMs, which is related to the difference in the primary energies of the electrons used in both cases (1 keV vs. 10 eV).[28]

Whereas the decrease of protein-layer thickness is steadily on the low-dose side of the trenches (phase B), the situation is more complex on the other side of these dips. Following the minimum of protein layer thickness, the resistance to protein adsorption becomes worse, until a certain level is reached at which the exchange-hindering cross-linking and exchange-promoting defect formation appear to achieve a dynamic equilibrium (phase C). At very high doses (greater than 2 mC cm^{-2}) the damage seems to become so significant that more adsorption places for the EG7UT become available, which slightly increases the resistance to protein adsorption. For future applications, we propose to stay within the dose

range of phase B, for which the area dose and the protein resistance correlate positively.

In conclusion, we have shown that gradients of protein affinity can be fabricated in a controllable manner on the micrometer length scale using a combination of IPER and EBL. The mechanism behind IPER is a creation of irradiation-induced defects, which promote the subsequent exchange reaction with potential molecular substituents, in this particular study a protein resistant ethylene glycol terminated thiol. The extent of exchange can be precisely tuned by dose selection in a defined dose range determined by the competition between the defect creation and cross-linking. The use of EBL permits the inherent generation of gradients with unprecedented complexity and reproducibility. We expect that this technology can be used for the fabrication of protein chips, and to study the influence of highly defined gradients on the morphogenesis, alignment, and chemotaxis of living cells.

Received: February 19, 2008
Revised: June 17, 2008
Published online: August 14, 2008

Keywords: bioresistance · photoelectron spectroscopy · protein adhesion · surface analysis · surface chemistry

[1] B. Brandley, J. H. Sharper, R. L. Schnaar, *Dev. Biol.* **1990**, *140*, 161.
[2] N. J. Sniadecki, R. A. Desai, S. A. Ruiz, C. S. Chen, *Ann. Biomed. Eng.* **2006**, *34*, 59.
[3] R. H. Terrill, K. M. Balss, Y. Zhang, W. P. Bohn, *J. Am. Chem. Soc.* **2000**, *122*, 988.
[4] K. M. Balss, B. D. Coleman, C. H. Lansford, R. T. Haasch, P. W. Bohn, *J. Phys. Chem. B* **2001**, *105*, 8970.
[5] N. V. Venkataraman, S. Zürcher, N. D. Spencer, *Langmuir* **2006**, *22*, 4184.
[6] T. Kraus, R. Stutz, T. E. Balmer, H. Schmid, L. Malaquin, N. D. Spencer, H. Wolf, *Langmuir* **2005**, *21*, 7796.
[7] M. K. Chaudhury, G. M. Whitesides, *Science* **1992**, *256*, 1539.
[8] B. Zhao, *Langmuir* **2004**, *20*, 11748.
[9] B. Liedberg, P. Tengvall, *Langmuir* **1995**, *11*, 3821.
[10] M. Riepl, M Östblom, I. Lundström, S. C. T. Svensson, A. W. D. van der Gon, M. Schäferling, B. Liedberg, *Langmuir* **2005**, *21*, 1042.
[11] S. K. W. Dertinger, D. T. Chiu, N. L. Jeon, G. M. Whitesides, *Anal. Chem.* **2001**, *73*, 1240.
[12] X. Y. Jiang, Q. Xu, S. K. W. Dertinger, A. D. Stroock, T. Fu, G. M. Whitesides, *Anal. Chem.* **2005**, *77*, 2338.
[13] R. R. Fuierer, R. L. Carroll, D. L. Feldheim, C. B. Gorman, *Adv. Mater.* **2002**, *14*, 154.
[14] K. Loos, S. B. Kennedy, N. Eidelman, Y. Tai, M. Zharnikov, E. J. Amis, A. Ulman, R. A. Gross, *Langmuir* **2005**, *21*, 5237.
[15] P. Burgos, M. Geoghegan, G. J. Leggett, *Nano Lett.* **2007**, *7*, 3747.
[16] C. B. Herbert, T. L. McLernon, C. L. Hypolitel, D. N. Adams, L. Pikusl, C.-C. Huang, G. B. Fields, P. C. Letourneau, M. D. Distefano, W.-S. Hu, *Chem. Biol.* **1997**, *4*, 731.
[17] N. Ballav, A. Shaporenko, A. Terfort, M. Zharnikov, *Adv. Mater.* **2007**, *19*, 998.
[18] N. Ballav, A. Shaporenko, S. Krakert, A. Terfort, M. Zharnikov, *J. Phys. Chem. C* **2007**, *111*, 7772.
[19] N. Ballav, T. Weidner, K. Rößler, H. Lang, M. Zharnikov, *ChemPhysChem* **2007**, *8*, 819.
[20] R. Klauser, M.-L. Huang, S.-C. Wang, C.-H. Chen, T. J. Chuang, A. Terfort, M. Zharnikov, *Langmuir* **2004**, *20*, 2050.
[21] R. Klauser, I.-H. Hong, S.-C. Wang, M. Zharnikov, A. Paul, A. Gölzhäuser, A. Terfort, T. J. Chuang, *J. Phys. Chem. B* **2003**, *107*, 13133.
[22] N. J. Brewer, S. Janusz, K. Critchley, S. D. Evans, G. J. Laggett, *J. Phys. Chem. B* **2005**, *109*, 11247.
[23] Y. Ito, M. Heydari, A. Hashimoto, T. Konno, A. Hirasawa, S. Hori, K. Kurita, A. Nakajima, *Langmuir* **2007**, *23*, 1845.
[24] I. S. Maeng, J. W. Park, *Langmuir* **2003**, *19*, 4519.
[25] E. Garand, P. A. Rowntree, *J. Phys. Chem. B* **2005**, *109*, 12927.
[26] M. Zharnikov, M. Grunze, *J. Vac. Sci. Technol. B* **2002**, *20*, 1793.
[27] K. L. Prime, G. M. Whitesides, *J. Am. Chem. Soc.* **1993**, *115*, 10714.
[28] M. Steenackers, A. Küller, N. Ballav, M. Zharnikov, M. Grunze, R. Jordan, *Small* **2007**, *3*, 1764.

